Journal of Civil Engineering and Applications

E-ISSN: 2707-8396
P-ISSN: 2707-8388
JCEA 2024; 5(1): 23-32
Received: 15-11-2023
Accepted: 20-12-2023

HHM Darweesh
Department of Refractories, Ceramics and Building Materials, National Research Centre, Cairo, Egypt

Corresponding Author:
HHM Darweesh
Department of Refractories, Ceramics and Building Materials, National Research Centre, Cairo, Egypt

Reactive magnesia Portland blended cement pastes

HHM Darweesh

Abstract
Physical and mechanical properties of ordinary Portland cement (OPC) blended with magnesium oxide (MgO) cement pastes (OPC/MgO) have been studied. Results showed that all physical and mechanical properties of OPC cement are improved and enhanced by the incorporation of the reactive MgO up to 2.5 wt. % and tended to be stable at 3.0 wt. % because the water curing process significantly increased the reaction degree of the used MgO, but with any further increase of MgO content › 3.0 wt. %, negative results are obtained. It is good mention that though OPC/MgO cement needed high water requirements to achieve the best results, both total porosity and water absorption decreased at all curing conditions. This reflected positively on bulk density and mechanical strengths. MgO could be used as a useful and simple binder at normal conditions. The optimum amount of the added MgO is between 2.5-3.0 wt. % at which acceptable porosity, bulk density, water absorption, and mechanical properties were achieved, but more than this ratio must be avoided due to its adverse effects.

Keywords: Cement, MgO, hydration, porosity, density, strength

1. Introduction
Magnesia (MgO) is too rare in nature. So, it is often produced either by the calcination of natural magnesite ($MgCO_3$) or from the deposits of dolomite, $CaMg(CO_3)_2$] or $Mg(OH)_2$ precipitated from seawater or generally magnesium-bearing brines [1-3]. Reactivity of MgO tends to decrease with the increase of calcination temperature. Magnesia has a number of categories, namely, light-burned or MgO (LB-MgO, 700-1000 °C), hard-burned MgO (HBMgO, 1000-1400 °C), dead-burned MgO (DB-MgO, 1400-2000 °C), and fused magnesia (F-MgO, >2800 °C) [4, 5]. All MgO types can be used as a main component to make MgO-based cements. Blends of LB-MgO powder with oxysalts, e.g. chlorides and sulfates or reactive silica have been widely studied to produce magnesium oxychloride cements, magnesium oxysulfate cement or magnesium silicate hydrate cements [6-8]. Magnesium phosphate cements (MPC) is made from DB-MgO and phosphoric acid [9, 10]. MgO plays an important role in a variety of cementitious material systems, e.g. alkali-activated slag cement and Ca-bearing cements. HB-MgO is generally used as an expansive agent to compensate for the thermal shrinkage of mass concrete due to its rapid expansion in early stages [11, 12]. LB-MgO is also used to improve the carbonation resistance of alkali-activated slag or calcium sulfoaluminate cement [13, 14]. MgO is often used as a vital component for diverse cementitious materials, and it has been tried as a binder alone. Reactive MgO cement (RMC) is considered to be a potential sustainable alternative to Portland cement, because it gains strength through hydration and carbonation, which allows for permanent sequestration of CO_2 into its carbonation phases, thereby reducing CO_2 emissions from the life cycle [15, 16]. Strength source of RMC is the formation of hydrated magnesium carbonates with network structure and the reduction of porosity [17-20]. RMC is confined to pre-casting applications, e.g. masonry blocks, roof tiles, and bricks [21]. MgO binder would have greater potential value if cured under normal conditions rather than accelerated carbonation. There are a mortar for internal walls, a binder for refractory castables and repairing materials for historical buildings. But unfortunately, MgO alone has never been explicitly considered as a useful binder under ambient curing conditions. Air-cured samples of pure pastes of MgO and water often give very limited strength [14, 21-24]. In ambient conditions, RMC with accelerated carbonization conditions, researchers have listed the compressive strength to be 5 MPa or little more [25-28]. Some slightly higher strength occurred in specimens with high reaction degree or high relative humidity. This can be explained by the reactive MgO has high water demand and the primary phase formed is brucite, $Mg(OH)_2$, which is less effective at reducing porosity and providing binding ability [23, 29]. Compaction moulding and curing on 98% RH were used to reduce the porosity and increase the reaction degree.

This resulted in higher compressive strength of about 20 MPa [30]. In spite of the relatively low strength of MgO-H_2O system, MgO still exhibited some properties as a binder under ambient condition. In fact, the formation of hydration and carbonation products, microstructure and strength development of MgO systems are affected by several factors, e.g. reactivity of MgO, w/c-ratio, curing conditions, transport and concentration of CO_2 [2, 31, 32]. Adjustment of curing process or optimization of w/c ratio has been reported to effectively enhance the mechanical and microstructural properties of MgO systems at elevated CO_2 concentration [31, 33].

Because of the low rate and degree of MgO hydration under ambient conditions, large amounts of residual MgO may continue hydrate into $Mg(OH)_2$, which could potentially bring about volume instability of MgO binder [11, 12, 34]. In this context, cementitious and hardening properties of MgO under ambient curing conditions were evaluated for construction application use. To illustrate the inherent cementing capacity of MgO, paste specimens were prepared with OPC/MgO. This work could provide a better understanding of the ability of MgO to harden and gain significant strength under typical exposure conditions. Physical and mechanical properties were studied.

2. Materials and Methodology

2.1 Raw Materials

The used raw materials in this study are ordinary Portland cement (OPC) and magnesium oxide (MgO). The OPC sample (OPC Type I- CEM I 42.5 R) was delivered from Sakkara cement factory, Giza, Egypt, while MgO was supplied by El-Gomhoria Company for Chemicals, Ramsis Street, Cairo, Egypt. MgO was obtained by the calcination of magnesite ($MgCO_3$) at 1400 ℃ for 5 hours. The surface area or fineness of OPC and MgO samples was 3500 and 4050 cm^2/g, respectively which was measured by Air Permeability Apparatus [35]. Chemical composition measured by X-ray fluorescence (XRF) of OPC and MgO is recorded in Table 1. Table 2 indicates the mineralogical composition of the OPC sample. The specific gravities of OPC and MgO as measured with a Le Chatelier flask were 3.15 and 2.93 g/cm^3, respectively. Table 2 shows the Mineralogical composition of OPC sample, while Table 3 indicates the physical properties of the raw materials.

Table 1: Chemical composition of the OPC and MgO samples, mass%.

Oxides Materials	SiO_2	Al_2O_3	Fe_2O_3	CaO	MgO	MnO	P_2O_5	Na_2O	K_2O	SO_3	LOI
OPC	20.12	5.25	1.29	63.13	1.53	0.03	0.02	0.61	0.29	237	2.64
MgO	3.08	0.48	0.46	2.19	92.84	0.05	0.16	-----	0.04	0.03	2.81

Table 2: Mineralogical composition of the OPC sample, wt. %.

Phase Material	C_3S	β-C_2S	C_3A	C_4AF
OPC	47.94	29.27	5.82	11.68

Table 3: Physical properties of the raw materials, wt. %

Properties Materials	Specific gravity	Density, g/cm^3	Blaine surface area, cm^2/g
OPC	3.15	1445	3500
MgO	2.79	1313	4050

2.2 Sample preparation

Cement pastes were prepared from OPC and MgO, which was added with various ratios as 0.0, 0.5, 1.0, 1.5, 2.0, 2.5, 3.0, 3.5 and 4.0 wt. % and are given the symbols M0, M1, M2, M3, M4, M5, M6, M7 and M8, respectively.

To obtain a suitable paste, 1% polycarboxylate ether (PCE) superplasticizer was added into the mixing water. Deionized water was used to eliminate the effect of CO_2 in water. After mixing, the pastes were cast into 2.5 × 2.5 × 2.5 cm^3 for total porosity (TP), bulk density (BD), water absorption (WA) and compressive strength (CS), but 2.5 × 2.5 × 7 cm^3 stainless steel moulds for flexural strength (FS), respectively.

The specimens were demoulded in the next day and soon subjected to natural water curing in the laboratory for 1, 3, 7, 28 and 90 days.

2.3 Methodology

Water of consistency (WC) and setting times as initial setting time (IST) and final setting time (FST) of cement pastes were assessed by needles penetration resistance of Vicat Apparatus [36-38]. Water of consistency was measured from the following relation:-

$$WC, \% = A / C \times 100 \quad (1)$$

Where, A is the amount of water taken to produce a suitable paste, C is the amount of cement (300 g). Physical properties as TP, BD and WA [39, 40] are determined from the following equations:-

$$WA, \% = (W1–W2) / (W3) \times 100 \quad (2)$$

$$BD, g/cm^3 = (W1) / (W1–W2) \quad (3)$$

$$\varepsilon = (0.99 \times We \times BD) / (1+Wt) \quad (4)$$

Where, W1, W2, W3, ε, We and 0.99 are the saturated, suspended, dry weights, total porosity, free or evaporable water content and specific volume of free water, respectively. Mechanical properties in terms of flexural strength (FS) and compressive strength (CS) [41, 42] are also measured from the following equations:-

$$FS = 3 (PL) / 2 (b) (d) / 10.2 \text{ Mpa} \quad (5)$$

$$CS = L (KN)/Sa (cm^2) KN/m^2 \times 102 (Kg/cm^2)/10.2 (MPa) \quad (6)$$

Where, L: load taken, Sa: surface area, P: bean or loading of rupture, b: width, d: thickness. The FS could be carried out using the three point adjustments system (Fig. 1).

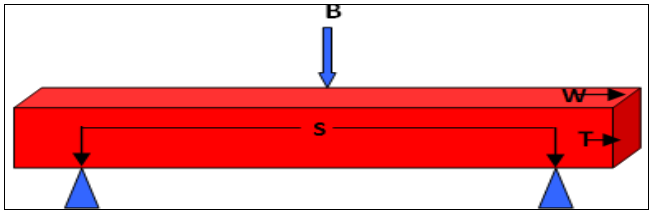

Fig 1: Schematic diagram of bending strength, B: Beam or loading of rupture, S: Span, W: Width and T: Thickness.

The loading was applied perpendicular to the direction of the upper surface of the cubes. Three samples were tested for each batch at all ages of hydration and the mean value was considered. The bound water content (Bn) of the hydrated samples pre-dried at 105 ºC for 24 hours was determined on the bases of ignition loss at 1000 ºC for 30 minutes [36, 39, 43-45] from the equation:

$$Bn, \% = W1-W2/W2 \times 100 \quad (7)$$

Where Bn, W1 and W2 are combined water content, weight of sample before and after ignition, respectively.

3. Results and Discussion

3.1 Water consistency and setting time

Figure 2 shows water of consistency and setting times (initial and final) of OPC/MgO cement pastes with different ratios of MgO. Water of consistency of the blank is 28.65% which increased gradually with the increase of MgO content. This is mainly attributed to the fact that MgO likes water too much to be reactive, i.e. magnesia cement needs many amount of water to normally hydrate with cement [43]. Both initial and final setting times of the reference sample (M0) are 112 and 131 min., respectively, which were becoming gradually longer than those of M0 [46]. Results of setting time suggested that the used superplasticizer does not cause a strong water reduction. This may be due to the longer w/c ratio and low free water evaporation during setting [43, 47].

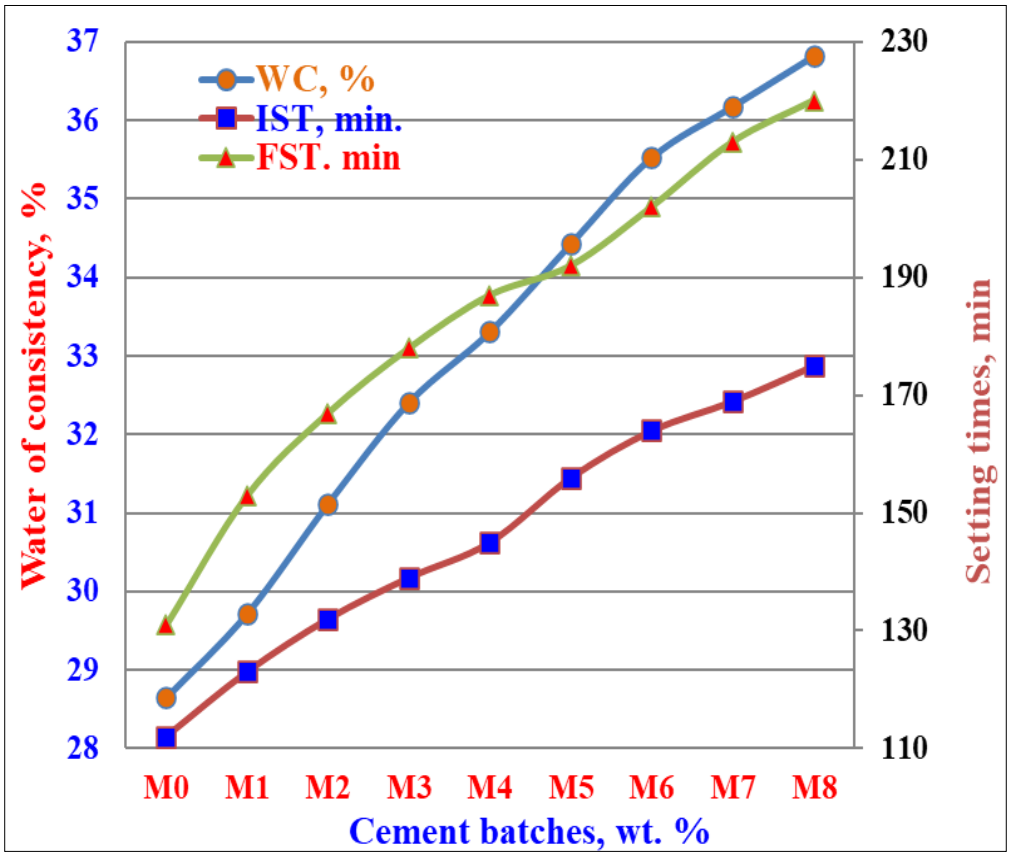

Fig 2: Water of consistency and setting times (initial and final) of the various cement batches incorporating different ratios of MgO.

3.2 Bound water content

Results of bound water content (BW) of cement pastes incorporated different ratios of MgO hydrated up to 90 days are illustrated in Fig. 3. As it is clear, the BW contents of the blank cement batch (M0) sharply increased as the curing times proceeded up to 90 days. This is principally contributed to the normal hydration process, where as the major cement phases were being in contact with water, it soon reacted with water to form hydration products [15, 18, 29, 40]. The formed hydration products immediately deposited in the available open pore structure till seemed to be filled with it. Hence, the total porosity decreased and the bulk density improved and enhanced. The BW contents of other cement batches incorporating different ratios of MgO displayed the same trend as M0, where it also increased till 3.0 wt. % MgO (M1 and M6), and then decreased with the excess MgO content (M7 and M8). The increase of BW contents is mainly due to that nanograin size particles of MgO always reacted with water forming another hydration products as $Mg(OH)_2$. This in turn precipitated inside the pore volume leading to its decrease. Moreover, the reactive MgO led to improve and increase the reactivity of cement phases. The decrease of BW contents is essentially contributed to the higher concentration of $Mg(OH)_2$ which tended to reopen the pores [21, 43, 47]. As a result, the larger amounts of MgO are undesirable.

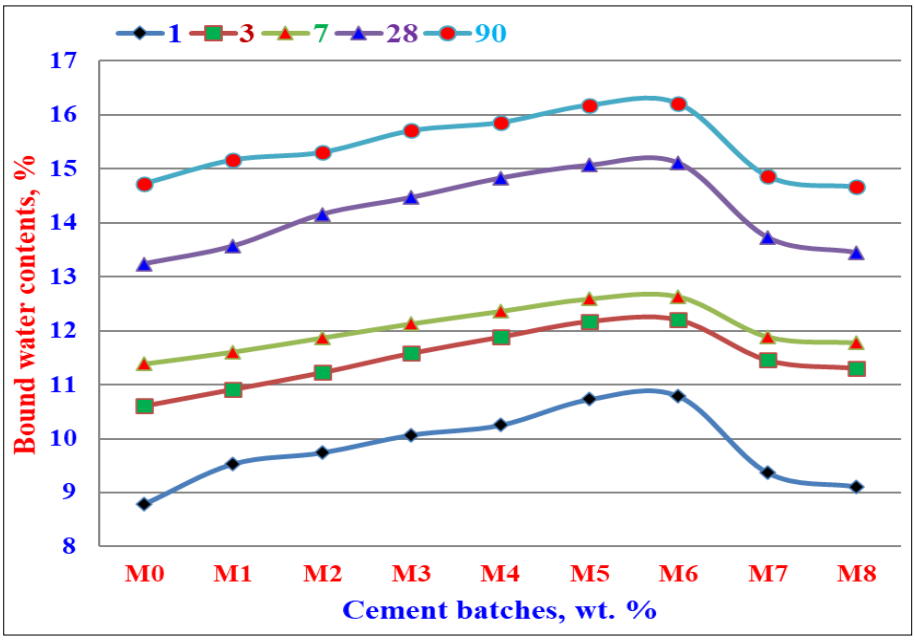

Fig 3: Bound water content of the various cement batches incorporating different ratios of MgO hydrated up to 90 days.

3.3 Total porosity and Bulk density

The total porosity (TP) and bulk density of cement pastes incorporated different ratios of MgO hydrated up to 90 days are illustrated in Fig. 4 and 5, respectively. Results showed that the TP slightly decreased as the MgO ratio increased in the specimens up to 2.5 wt. % MgO (M6), and then it remained relatively constant up to 3.0 wt. %. This essentially due to that the degree of the reaction of MgO with the various constituents of the cement increased with the curing time. Moreover, the decrease of the TP due to the increase of MgO ratio increased the compaction of the hardened cement paste samples, which decreased the TP. This in turn reflected positively on the bulk density, i.e. it improved and enhanced. Also, the dispersive effect of both MgO and the used admixture to the cement powder helped more in the hydration process [43-51]. Hence, the specimens showed a minimum TP and maximum BD, i.e. for M5 and M6 nearly recorded the lowest porosity after 90 days hydration (20.11 and 20.18%) and the highest density (2.2448 and 2.2451 g/cm^3), which might be advantageous to the diffusion of CO_2 in specimens and eventually led to effective strength improvements [52-54]. The further increase in MgO ratio (M7 and M8) created more open pores, and so lowered the bulk density due to the increase of TP. The increase of TP can be explained by the gradual evaporation of free water within samples during hardening [47, 51-53]. Although water curing promotes the hydration of MgO, the subsequent formation of more Mg $(OH)_2$ and reduction of porosity, the formed $Mg(OH)_2$ can be in effective contact with CO_2 in air and so it promoted the strength development. Extra water provided by wet environments led to improve and enhance the reaction products that deposited and filled the available pore space. Therefore, the TP reduced, while the bulk density increased. The optimum cement batch is that contains 2.5-3.0 wt % MgO (M5 and/or M6) noticing that the higher amounts of MgO (M7 and M8) › 3.0 wt. % must be prevented.

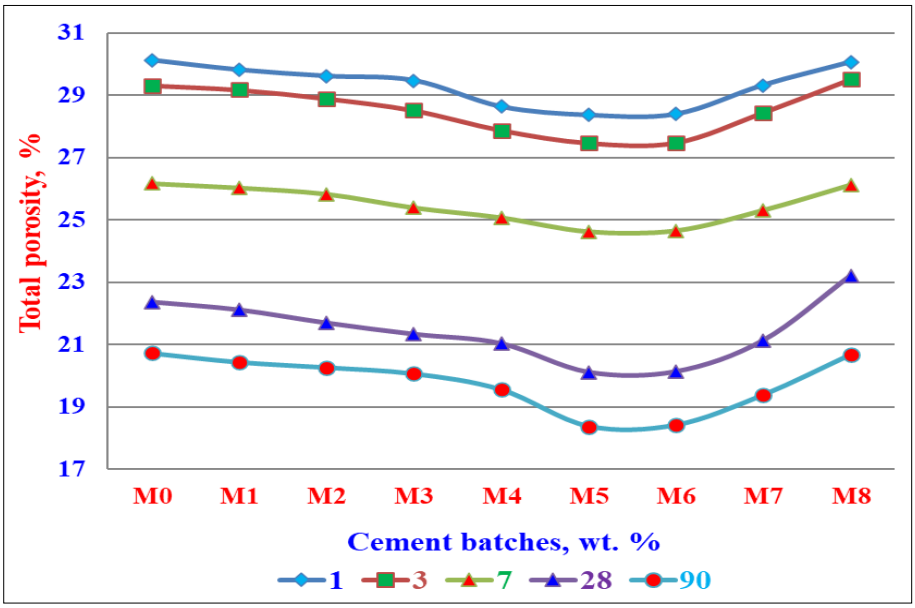

Fig 4: Total porosity of the various cement batches incorporating different ratios of MgO hydrated up to 90 days.

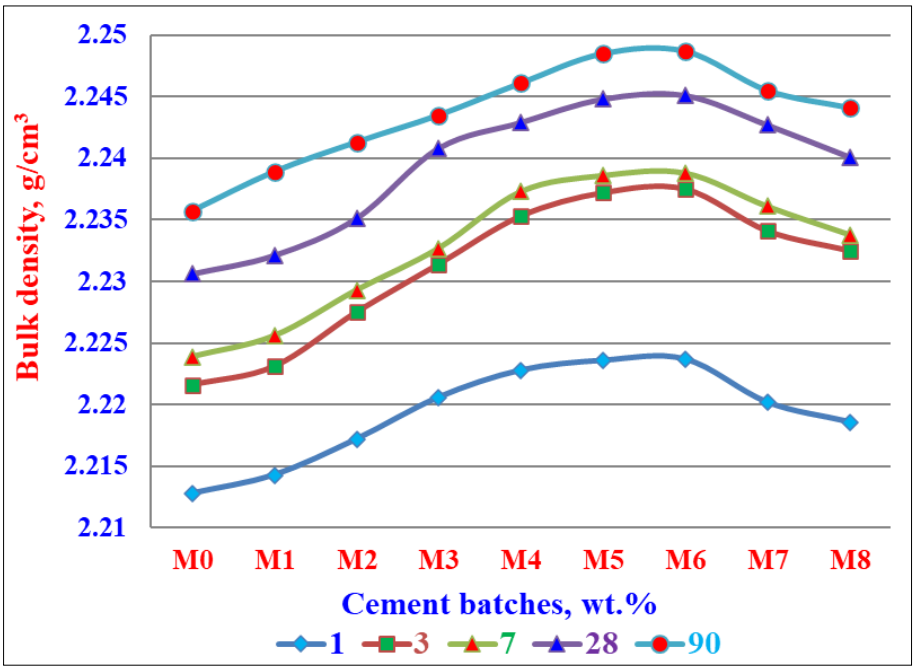

Fig 5: Bulk density of the various cement batches incorporating different ratios of MgO hydrated up to 90 days.

3.4 Water absorption: Water absorption (WA) of OPC/MgO cement pastes with varying proportions of MgO hydrated up to 90 days is shown in Fig. 6. The WA of the control batch (M0) gradually decreased as the hydration ages progressed up to 90 days. This is attributed to the normal hydration process, where the major phases of the cement reacted with water forming hydration products. The formed hydration products soon filled the pore system of the hardened samples. This in turn decreased the total porosity and therefore the WA decreased little by little [15, 18, 28, 38]. The WA of the cement batches containing various ratios of MgO (M1-M6) also decreased with the curing times up to 90 days, but only up to 3.0 wt. % (M6). With any further increase of MgO content (M7 and M8), the WA behaved adversely, i.e. the WA tended to increase. The decrease of WA is mainly contributed to the gradual decrease of porosity due to the presence of reactive MgO that reacted with water forming Mg $(OH)_2$ and moreover the double dispersion effect of both MgO and the used admixture which promoted the hydration process where M6 recorded the minimum WA value [50, 51]. The WA is also related to surface porosity as well as structural pores [51]. On contrast, with any other addition of MgO (M7 and M8), the WA adversely affected, i.e. it suddenly increased [52, 53]. This may be due to the used higher w/c ratio [51-54]. So, it could be concluded that the optimum cement batch is M6 that is containing 3.0 wt. % MgO which achieved the higher values of BD and the lower values of TP and WA.

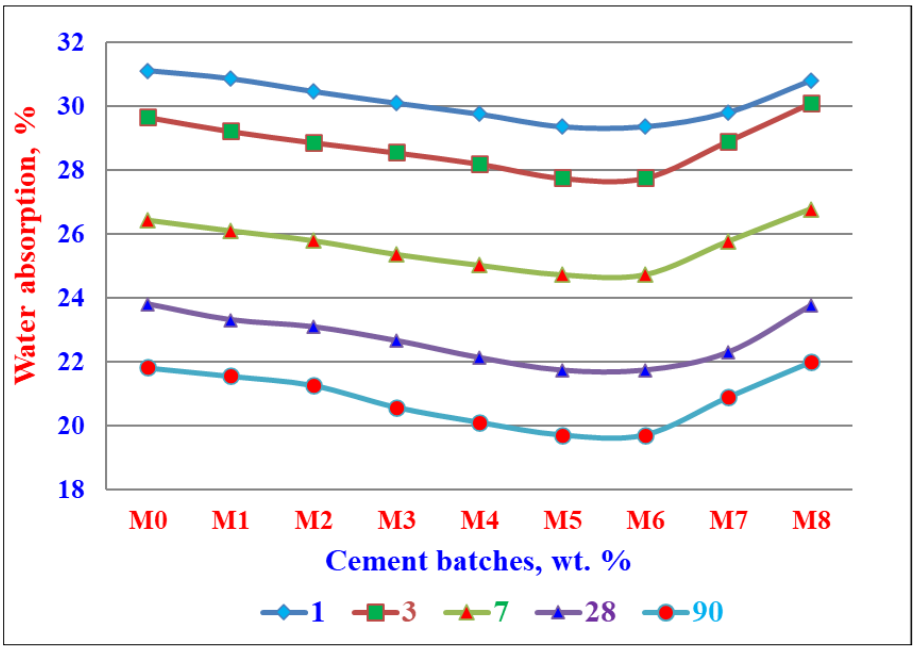

Fig 6: Water absorption of the various cement batches incorporating different ratios of MgO hydrated up to 90 days.

3.5 Compressive strength

Figure 7 indicates the compressive strength (CS) of OPC/MgO cement pastes with varying proportions of MgO cured up to 90 days. Large strength gain was observed for

all samples during 28-90 days, i.e. the CS of OPC/MgO cement pastes (M0) increased with the increase of MgO content and curing time up to 90 days. This was continued up to 2.5-3.0% MgO (M5 and M6), but then was decreased with any further increase of MgO content (M7 and M8). The CS of the cement pastes M1-M6 achieved CS higher than those of the blank (M0) as in some previous studies [47, 56, 57]. Significant high difference in strength gain can be attributed to that the used MgO, which was burned at a temperature of 1400 ℃, had a relatively higher reactivity [58-60]. Also, the quick and continuous hydration of MgO may be positive for the diffusion of atmospheric CO_2 in the specimens. So, the rapid hydration of MgO and formation of Mg $(OH)_2$ could be densificated the specimens. In addition, the hydration over time could induce a denser structure and higher strength of MgO based cementitious materials [59, 60]. Under water curing condition, quite acceptable CS after 90 days was obtained for M6 that exhibited the highest CS (60.81 MPa). On the other side however, lowest CS could be obtained with M8 (56.87 MPa). This may be attributed to the high rate of water retention of cement specimens, that limited the carbonation of Mg $(OH)_2$ before demoulding. Thus, a slight downward strength development trend was observed. The continuous formation of Mg $(OH)_2$ occurred in samples had led to the formation of micro-cracks and a subsequent reduction in compressive strength [35]. This demonstrated that the porosity re-increased further under water curing, and then hindered the CO_2 diffusion in the cores of specimens. The nanofine particles could be reduced the volume of porous hardened pastes, whereas the less fine particles can absorb and store a certain amount of water, which promotes the hydration of MgO after setting, and provides more channels for the diffusion of CO_2 within specimens. Therefore, the use of magnesia as a binder may be a better way for cement pastes. However, the strength development of OPC/MgO pastes is too high under water curing conditions. This could be explained as MgO low reaction degree and insufficient products to bind large particles [61-63]. The optimum cement batch is that contains 2.5-3.0 wt % MgO (M5 and/or M6) noticing that the higher amounts of MgO › 3.0 wt. % (M7 and M8) must be is avoided.

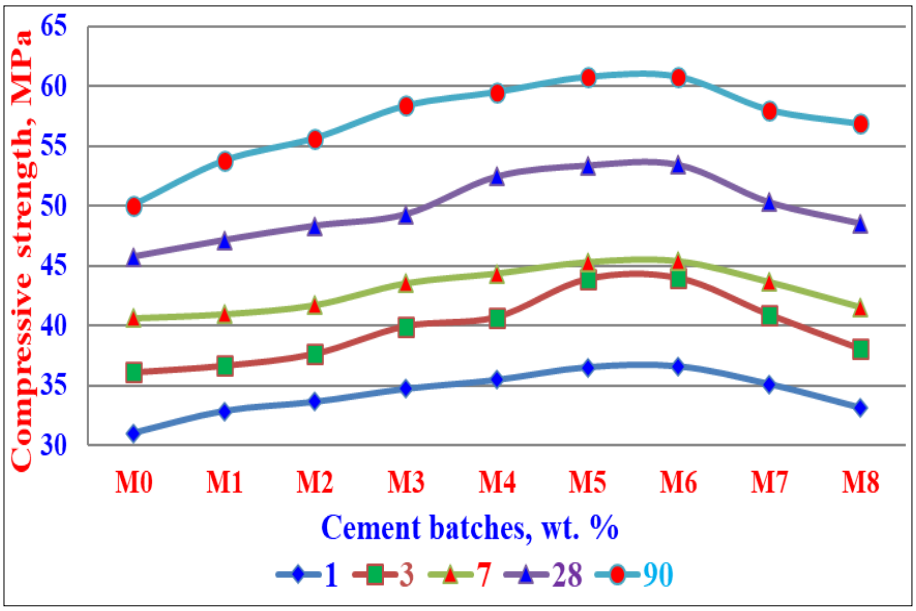

Fig 7: Compressive strength of the various cement batches incorporating different ratios of MgO hydrated up to 90 days.

3.6 Flexual strength

Flexural strength (FS) of OPC/MgO cement pastes with varying ratios of MgO cured up to 90 days is shown in Fig. 8. The FS values improved and enhanced with curing times up to 90 days according to the normal hydration process [39, 64]. On the other hand, the FS also increased with MgO content. This continued up till 2.5 wt. % MgO (M5) at which it remained stable at 3.0 wt. % MgO (M6). But then, the FS values were gradually declined and adversely affected with any further increase in MgO content (M7 and M8). The increase of FS is mainly due to that the MgO highly reacted with water to form additional hydration products as Mg $(OH)_2$, i.e. the degree of reactivity of MgO increased with curing times [65, 66], which soon deposited in the internal still open pores. This in turn increased its densification, i.e. form dense structure. So, the total porosity decreased. This would be reflected positively on the bulk density and thereafter on the FS. Moreover, the non-hydrated nano-grain size particles of MgO could be filled the open pores. Therefore, the total porosity decreased more, and so all these improvements could be reflected positively on the FS [58-60]. The decrease of FS is only contributed to the larger formation of Mg $(OH)_2$ which led to create internal minor cracks which weakened the hardened cement pastes that reflected negatively on the FS [35, 59-62]. Also, this may be attributed to the high rate of water retention of samples, that limited the carbonation of $Mg(OH)_2$ before demoulding [66, 67]. It is postulated that the continuous formation of $Mg(OH)_2$ occurred in the samples without sufficient w/c ratio, resulted in the formation of microcracks and a subsequent reduction in flexural and compressive strengths [68]. Hence, the optimum cement batch is that contains 2.5-3.0 wt % MgO (M5 and/or M6) noticing that the higher amounts of MgO › 3.0 wt. % is undesired (M7 and M8).

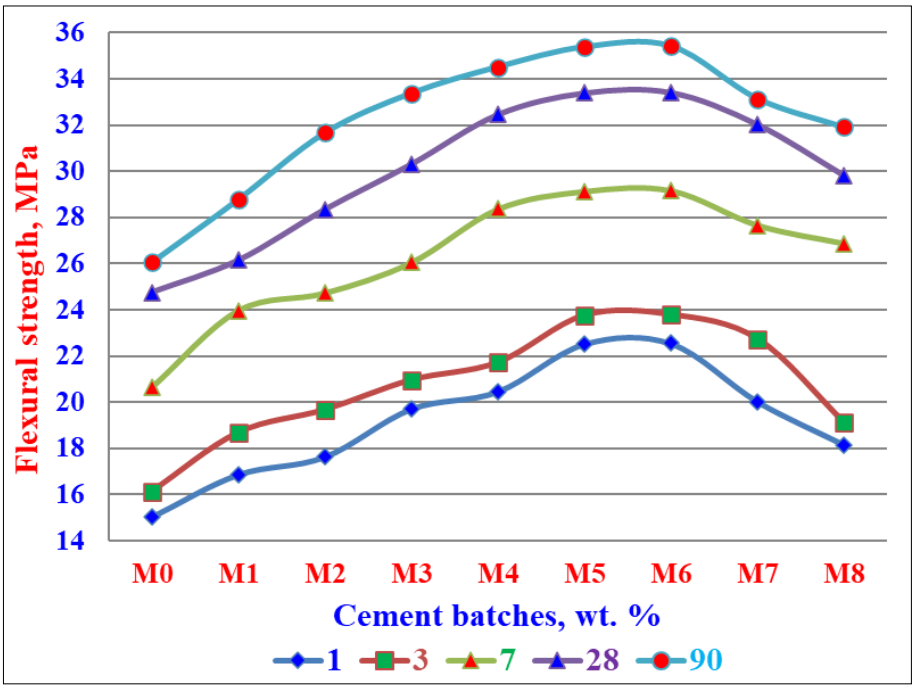

Fig 8: Flexural strength of the various cement batches incorporating different ratios of MgO hydrated up to 90 days.

4. General Discussion

It is clear that the initial hydration reaction among MgO and H_2O where MgO particles are completely wrapped by water, i.e. MgO can directly hydrate to form Mg $(OH)_2$ as follows:

$$MgO + H_2O \rightarrow Mg(OH)_2 \quad (8)$$

The degree of reactivity of MgO improved and enhanced with curing times. The low solubility of MgO and the precipitation of Mg $(OH)_2$ surrounded the MgO particles would inhibit its further hydration [69, 70]. A combination of MgO and Mg $(OH)_2$ is thus maintained in the solid phases. MgO and/ or Mg $(OH)_2$ can potentially form a wide range of $MgCO_3$ and hydroxyl-carbonates [66, 71, 72]. These products can be formed spontaneously under natural conditions. Although both MgO and Mg $(OH)_2$ can be carbonated, the growth rate of these is strongly controlled by kinetics. Also, the formation of $MgCO_3$ is inhibited by the high hydration energy of Mg^{2+} [67], and the carbonation products are usually hydrated magnesium carbonates ($MgO/MgCO_3/H_2O$) or (MCH) instead of $MgCO_3$ alone. Furthermore, the carbonation of MgO to form MCH is evidently affected by temperature, relative humidity (RH), partial pressure of CO_2 and reactivity of MgO [65, 67, 68]. Brucite, Mg $(OH)_2$ is the main crystalline reaction product, along with residual periclase (MgO) observed in all samples, indicating that MgO can hydrate to form Mg $(OH)_2$. This is due to the higher reaction degree of MgO because of both its higher reactivity and greater w/c ratio [73-75].

5. Conclusion

The incorporation of reactive magnesia (MgO) into a cementitious material initiated and promoted its physical and mechanical properties. Though the OPC/MgO cement needed more water requirements, the added water-reducing admixture lowered it to some extent. MgO increased the water of consistency and setting times. The addition of the very fine or nanoMgO to cement increased its compaction due to the deposition of the formed hydration products into the pore structure. This in turn decreased the total porosity, and hence increased the bulk density. The optimum MgO content at which the physical and mechanical properties are being the best is between 2.5--3.0 wt. %. The larger quantity › 3.0 wt. % must be eliminated. After 90 days, the optimum batch achieved TP, BD, WA, FS and CS as 17.74%, 2.2507 g/cm^3, 19,71%, 36.18 MPa and 63.08 MPa, respectively. The hydrated MgO fills the voids of the hardened samples and improves the early-age strength. The non-hydrated MgO also precipitated into the empty voids. At all, the optimum batch exhibited the higher values of bulk density, flexural and compressive strengths at all curing times, while recorded the lower values of total porosity and water absorption. All results of M6 is nearly constant as M5, i.e. it exhibited nearly the same values. So, the used reactive MgO could be used as a useful binder in the cementing materials. It is good mention that though the values of M7 and M8 decreased at all curing times than those of other batches, it still higher than those of the blank (M0).

6. Declaration of Competing Interest

Authors declare that they do not have any commercial or associative interest that represents a conflict of interest in connection with the work submitted.

7. Acknowledgments

Authors gratefully acknowledge the financial support of the National Research Centre.

8. Funding

This research article is self-sponsored.

9. References

1. Nobre J, Ahmed H, Bravo M, Evangelista L, de Brito J. Magnesia (MgO) production and characterization, and its influence on the performance of cementitious materials: A review. Materials. 2020;13(21):4752. https://doi.org/10.3390/ma13214752.
2. Panda B, Sonat C, Yang E, Tan MJ, Unluer C. Use of

magnesium-silicatehydrate (M-S-H) cement mixes in 3D printing applications. Cement and Concrete Composites. 2021;117:103901. https://doi.org/10.1016/j.cemconcomp.2020.103901.
3. Zhang G, Wang Q, Li Y, Zhang M. Microstructure and micromechanical properties of magnesium phosphate cement. Cement and Concrete Research. 2023;172:107227. https://doi.org/10.1016/j.cemconres.2023.107227.
4. Li Z, Chau CK. Influence of molar ratios on properties of magnesium oxychloride cement. Cement and Concrete Research. 2007;37:866-870. https://doi.org/10.1016/j.cemconres.2007.03.015.
5. Zhu J, Ye N, Liu J, Yang J. Evaluation on hydration reactivity of reactive magnesium oxide prepared by calcining magnesite at lower temperatures. Industrial & Engineering Chemistry Research. 2013;52:6430-6437. https://doi.org/10.1021/ie303361u.
6. Ruan S, Unluer C. Influence of mix design on the carbonation, mechanical properties and microstructure of reactive MgO cement-based concrete. Cement and Concrete Composites. 2017;80:104-114. https://doi.org/10.1016/j.cemconcomp.2017.03.004.
7. Zhang R, Bassim N, Panesar DK. Characterization of Mg components in reactive MgO-Portland cement blends during hydration and carbonation. Journal of CO_2 Utilization. 2018;27:518-527. https://doi.org/10.1016/j.jcou.2018.08.025.
8. Zhang T, Vandeperre LJ, Cheeseman CR. Formation of magnesium silicate hydrate (M-S-H) cement using sodium hexametaphosphate. Cement and Concrete Research. 2014;65:8-14. https://doi.org/10.1016/j.cemconres.2014.07.001.
9. Qiao F, Chau CK, Li Z. Property evaluation of magnesium phosphate cement mortar as patch repair material. Construction and Building Materials. 2010;24:695-700. https://doi.org/10.1016/j.conbuildmat.2009.10.039.
10. You C, Qian J, Qin J, Wang H, Wang Q, Ye Z. Effect of early hydration temperature on hydration product and strength development of magnesium phosphate cement (MPC). Cement and Concrete Research. 2015;78:179-189. https://doi.org/10.1016/j.cemconres.2015.07.005.
11. Mo L, Deng M, Tang M, Al-Tabbaa A. MgO expansive cement and concrete in China: past, present and future. Cement and Concrete Research. 2014;57:1-12. https://doi.org/10.1016/j.cemconres.2013.12.007.
12. Hay R, Celik K. Hydration, carbonation, strength development and corrosion resistance of reactive MgO cement-based composites. Cement and Concrete Research. 2020;128:105941. https://doi.org/10.1016/j.cemconres.2019.105941.
13. Seo J, Yoon HN, Kim S, Wang Z, Kil T, Lee HK. Characterization of reactive MgO-modified calcium sulfoaluminate cements upon carbonation. Cement and Concrete Research. 2021;146:106484. https://doi.org/10.1016/j.cemconres.2021.106484.
14. Dung NT, Hooper TJN, Unluer C. Improving the carbonation resistance of Na2CO3-activated slag via the use of reactive MgO and nucleation seeding. Cement and Concrete Composites. 2021;115:103832. https://doi.org/10.1016/j.cemconcomp.2020.103832.
15. Dung NT, Unluer C. Performance of reactive MgO concrete under increased CO_2 dissolution. Cement and Concrete Research. 2019;118:92-101. https://doi.org/10.1016/j.cemconres.2019.02.007.
16. Ruan S, Unluer C. Comparative life cycle assessment of reactive MgO and Portland cement production. Journal of Cleaner Production. 2017;137:258-273. https://doi.org/10.1016/j.jclepro.2016.07.071.
17. Hu Z, Chang J, Chen X, Guan Y, Bi W. Preparation of magnesium oxysulfate cement with semidry carbonation high calcium content light-burned magnesium (Ca-LBM). Construction and Building Materials Journal. 2023;408:133664. https://doi.org/10.1016/j.conbuildmat.2023.133664.
18. Dung NT, Unluer C. Development of MgO concrete with enhanced hydration and carbonation mechanisms. Cement and Concrete Research. 2018;103:160-169. https://doi.org/10.1016/j.cemconres.2017.10.011.
19. Bhagath Singh GVP, Sonat C, Yang EH, Unluer C. Performance of MgO and MgO-SiO_2 systems containing seeds under different curing conditions. Cement and Concrete Composites. 2020;108:103543. https://doi.org/10.1016/j.cemconcomp.2020.103543.
20. Dung NT, Unluer C. Carbonated MgO concrete with improved performance: the influence of temperature and hydration agent on hydration, carbonation and strength gain. Cement and Concrete Composites. 2017;82:152-164. https://doi.org/10.1016/j.cemconcomp.2017.06.006.
21. Guan Y, Chang J, Hu ZQ, Bi WL. Performance of magnesium hydroxide gel at different alkali concentrations and its effect on properties of magnesium oxysulfate cement. Construction and Building Materials. 2022;348:128669. https://doi.org/10.1016/j.conbuildmat.2022.128669.
22. Luo X, Li Y, Lin H, Li H, Shen J, Pan B, *et al*. Research on predicting compressive strength of magnesium silicate hydrate cement based on machine learning. Construction and Building Materials. 2023;406:13341. https://doi.org/10.1016/j.conbuildmat.2023.133412.
23. Hay R, Celik K. Hydration, carbonation, strength development and corrosion resistance of reactive MgO cement-based composites. Cement and Concrete Research. 2020;128:105941. https://doi.org/10.1016/j.cemconres.2019.105941.
24. Ma S, Akca AH, Esposito D, Kawashima S. Influence of aqueous carbonate species on hydration and carbonation of reactive MgO cement. Journal of CO_2 Utilization. 2020;41:101260. https://doi.org/10.1016/j.jcou.2020.101260.
25. Xiao X, Goh LX, Unluer C, Yang E. Bacteria-induced internal carbonation of reactive magnesia cement. Construction and Building Materials. 2021;267:121748. https://doi.org/10.1016/j.conbuildmat.2020.121748.
26. Dung NT, Unluer C. Sequestration of CO_2 in reactive MgO cement-based mixes with enhanced hydration mechanisms. Construction and Building Materials. 2017;143:71-82. https://doi.org/10.1016/j.conbuildmat.2017.03.038.
27. Jang H, So S, Lim Y, Carbonation, CO_2 sequestration, and physical properties based on the mineral size of light burned MgO using carbonation accelerator. Journal of Cleaner Production. 2022;379:134648. https://doi.org/10.1016/j.jclepro.2022.134648.

28. Ruan S, Unluer C. Effect of air entrainment on the performance of reactive MgO and PC mixes. Construction and Building Materials. 2017;142:221-232. https://doi.org/10.1016/j.conbuildmat.2017.03.068.
29. Wang L, Chen L, Provis JL, Tsang DCW, Poon CS. Accelerated carbonation of reactive MgO and Portland cement blends under flowing CO2 gas. Cement and Concrete Composites. 2020;106:103489. https://doi.org/10.1016/j.cemconcomp.2019.103489.
30. Kuenzel C, Zhang F, Ferr´ andiz-Mas V, Cheeseman CR, Gartner EM. The mechanism of hydration of MgO-hydromagnesite blends. Cement and Concrete Research. 2018;103:123-129. https://doi.org/10.1016/j.cemconres.2017.10.003.
31. Dung NT, Hooper TJN, Unluer C. Influence of CO_2 concentration on the performance of MgO cement mixes. Cement and Concrete Composites. 2021;115:103826. https://doi.org/10.1016/j.cemconcomp.2020.103826.
32. Winnefelda F, Epifaniaa E, Montagnarob F, Gartner EM. Further studies of the hydration of MgO-hydromagnesite blends. Cement and Concrete Research. 2019;126:105912. https://doi.org/10.1016/j.cemconres.2019.105912.
33. Soares EG, Castro-Gomes J. Carbonation curing influencing factors of carbonated reactive magnesia cements (CRMC) - a review. Journal of Cleaner Production. 2021;305:127210. https://doi.org/10.1016/j.jclepro.2021.127210.
34. Dung NT, Lesimple A, Hay R, Celik K, Unluer C. Formation of carbonate phases and their effect on the performance of reactive MgO cement formulations. Cement and Concrete Research. 2019;125:105894. https://doi.org/10.1016/j.cemconres.2019.105894.
35. ASTM C204-18e1. Standard Test Methods for Fineness of Hydraulic Cement by Air-Permeability Apparatus. ASTM International; c2018.
36. Darweesh HHM. Metakaolin Blended Cement Pastes. International Journal of Innovative Studies in Sciences and Engineering Technology (IJISSET). 2020;6(1):5-18. www.ijisset.org.
37. ASTM-Standards. Standard Test Method for Normal water of Consistency of Hydraulic Cement. 1993;C187-86:148-150.
38. ASTM-C191-92. Standard Test Method for Setting Time of Hydraulic Cement; c1993. p. 866-868.
39. Hewlett PC, Liska M. Lea's Chemistry of Cement and Concrete. Butterworth-Heinemann; c2017.
40. ASTM C642-13. Standard Test Method for Density, Absorption, and Voids in Hardened Concrete. ASTM International; c2013.
41. ASTM C348-21. Standard Test Method for Flexural Strength of Hydraulic-Cement Mortars. ASTM International; c2021.
42. ASTM C109 / C109M-20b. Standard Test Method for Compressive Strength of Hydraulic Cement Mortars. ASTM International; c2020.
43. Darweesh HHH. Influence of Some Soluble Polymer Admixtures on the Hydration and Strength Development of Portland Cement Pastes. Journal of Sustainable Materials Processing and Management. 2022;2(1):1-14.
44. Darweesh HHM. Effect of banana leaf ash as a sustainable material on the hydration of Portland cement pastes. International Journal of Materials Science. 2023;4(1):01-11.
45. Darweesh HHM. Utilization of Oyster Shell Powder for Hydration and Mechanical Properties Improvement of Portland Cement Pastes. Journal of Sustainable Materials Processing and Management. 2023;3(1):19-30.
46. Li Z, Qian J, Qin J, Hua Y, Yue Y, Tang H. Cementitious and hardening properties of magnesia (MgO) under ambient curing conditions. Cement and Concrete Research. 2023;170:107184.
47. Hay R, Peng B, Celik K. Filler effects of $CaCO_3$ polymorphs derived from limestone and seashell on hydration and carbonation of reactive magnesium oxide (MgO) cement (RMC). Cement and Concrete Research. 2023;164:107040.
48. Ma H, Zhang S, Feng J. Physicochemical properties of MgO-silica fume cementitious materials exposed to high temperatures. Journal of Building Engineering. 2022;50:104124.
49. Winnefeld F, Epifania E, Montagnaro F, Gartner EM. Further studies of the hydration of MgO-hydromagnesite blends. Cement and Concrete Research. 2019;126:105912.
50. Kuenzel C, Zhang F, Ferrandiz-Mas V, Cheeseman CR, Gartner EM. The mechanism of hydration of MgO-hydromagnesite blends. Cement and Concrete Research. 2018;103:123-129.
51. Wang E, Li X, Dai S, Li Z, Zhao T, Song B, *et al*. Research on the mechanism of a mixed collector onto magnesite surface to improve the flotation separation of magnesite from hornblende. Physical Chemistry Problems of Mineral Processing. 2021;57:125-138.
52. Chen X, Wu S. Influence of water-to-cement ratio and curing period on pore structure of cement mortar. Construction and Building Materials. 2013;38:804-812.
53. Kooshkaki A, Eskandari-Naddaf H. Effect of porosity on predicting compressive and flexural strength of cement mortar containing micro and nano-silica by multiobjective ANN modeling. Construction and Building Materials. 2019;212:176-191.
54. Yacoub A, Djerbi A, Fen-Chong T. The effect of the drying temperature on water porosity and gas permeability of recycled sand mortar. Construction and Building Materials. 2019;214:677-684.
55. Hay R, Khalil A, Otchere C, Alanis S, Celik K. Proportioning, carbonation, performance assessment, and application of reactive magnesium oxide cementbased composites with superplasticizers. Journal of Materials in Civil Engineering. 2023;35:04022405.
56. Das D, Rout PK. Synthesis of Inorganic Polymeric Materials from Industrial Solid Waste. Silicon. 2023;15:1771-1791.
57. Hay R, Otchere C, Kashwani G, Celik K. Recycling carbonated reactive magnesium cement (RMC) as building material. Journal of Cleaner Production. 2021;320:128838.
58. Dung NT, Unluer C. Potential additives for magnesia-based concrete with enhanced performance and propensity for CO_2 sequestration. Journal of CO_2 Utilization. 2022;56:101834.
59. Dung NT, Hoang T, Yang E, Chu J, Unluer C. New frontiers in sustainable cements: improving the performance of carbonated reactive MgO concrete via

microbial carbonation process. Cement and Concrete Research. 2022;356:129243.
60. Mi T, Yang E, Unluer C. Investigation of the properties of reactive MgO-based cements and their effect on performance. Cement and Concrete Composites. 2023;138:104984.
61. Angelin AF, Lintz RC, Gachet-Barbosa LA, Osorio WR. The effect of porosity on mechanical behavior and water absorption of an environmentally friendly cement mortar with recycled rubber. Construction and Building Materials. 2017;151:534-545.
62. Sonat C, Lim CH, Liska M, Unluer C. Recycling and reuse of reactive MgO cements - a feasibility study. Construction and Building Materials. 2017;157:172-181.
63. Yang Q, Gao X, Fang L, Zhang S, Cheng F. Controllable crystal growth of Mg (OH)2 hexagonal flakes and their surface modification using graft polymerization. Advanced Powder Technology. 2021;32:2634-2644.
64. Neville AM. Properties of Concrete. 5th edn, Longman Essex, UK; c2011.
65. Darweesh HHM. Water Permeability, Strength Development And Microstructure of Activated Pulverized Rice Husk Ash Geopolymer Cement. NanoNEXT. 2022;3(1):5-22.
66. Darweesh HHM. Geopolymer Cement Based on Bioactive Egg Shell Waste or Commercial Calcium Carbonates. Research & Development in Material science. 2022;17(1):1907-1916.
67. Sonat C, Lim CH, Liska M, Unluer C. Recycling and reuse of reactive MgO cements: A feasibility study. Construction and Building Materials. 2017;157:172-181. https://doi.org/10.1016/j.conbuildmat.2017.09.068.
68. Kumar S, Sonat C, Yang E, Unluer C. Performance of reactive magnesia cement formulations containing fly ash and ground granulated blast-furnace slag. Construction and Building Materials. 2020;232:117275. https://doi.org/10.1016/j.conbuildmat.2019.117275.
69. Dung NT, Unluer C. Carbonated MgO concrete with improved performance: the influence of temperature and hydration agent on hydration, carbonation and strength gain. Cement and Concrete Composites. 2017;82:152-164. https://doi.org/10.1016/j.cemconcomp.2017.06.006.
70. Ruan S, Unluer C. Comparative life cycle assessment of reactive MgO and Portland cement production. Journal of Cleaner Production. 2017;137:258-273. https://doi.org/10.1016/j.jclepro.2016.07.071.
71. Walling SA, Provis JL. Magnesium-based cements: a journey of 150 years, and cements for the future. Chemical Reviews. 2016;116(7):4170-4204. https://doi.org/10.1021/acs.chemrev.5b00463.
72. Shah V, Scott A. Use of kaolinite clays in development of a low carbon MgO-clay binder system. Cement and Concrete Research. 2021;144:106422. https://doi.org/10.1016/j.cemconres.2021.106422.
73. Nguyen H, Santos H, Sreenivasan H, Kunther W, Carvelli V, Illikainen M, *et al*. On the carbonation of brucite: Effects of Mg-acetate on the precipitation of hydrated magnesium carbonates in aqueous environment. Cement and Concrete Research. 2022;153:106696. https://doi.org/10.1016/j.cemconres.2021.106696.
74. Singh I, Hay R, Celik K. Recovery and direct carbonation of brucite from desalination reject brine for use as a construction material. Cement and Concrete Research. 2022;152:106673. https://doi.org/10.1016/j.cemconres.2021.106673.
75. Can S, Sariisik A, Uygunoğlu T. Effects of waste magnesia powder as partial cement replacement on self-compacting concrete. Advances in Cement Research; c2023. https://doi.org/10.1680/jadcr.22.00126.
76. Zhang K, Zhao H, Wang C, Bi J. Effect of magnesium hydroxide on the mechanical properties and pore structure of cement mortar after high temperature exposure. Developments in the Built Environment. 2024;17:100340. https://doi.org/10.1016/j.dibe.2024.100340.